ISTITUTO NAZIONALE DI FISICA NUCLEARE - ISTITUTO NAZIONALE DI FISICA NUCLEARE - ISTITUTO NAZIONALE DI FISICA NUCLEARE - ISTITUTO NAZIONALE DI FISICA NUCLEARE - ISTITUTO NAZIONALE DI FISICA NUCLEARE - ISTITUTO NAZIONALE DI

Laboratori Nazionali di Frascati

To be published in Nucl. Instr. & Meth.

LNF-90/032(P)
3 Maggio 1990

M. Taiuti, E. Durante, M. Anghinolfi, N. Bianchi, P. Corvisiero, E. De Sanctis, G. Gervino, C. Guaraldo, P. LeviSandri, V. Lucherini, L. Mattera, V. Muccifora, E. Polli, A.R. Reolon, G. Ricco, P. Rossi, M. Sansone, G.M. Urcioli, U. Valbusa, A. Zucchiatti:

THE ARGON CLUSTER-BEAM INSTALLED IN THE ADONE STORAGE RING

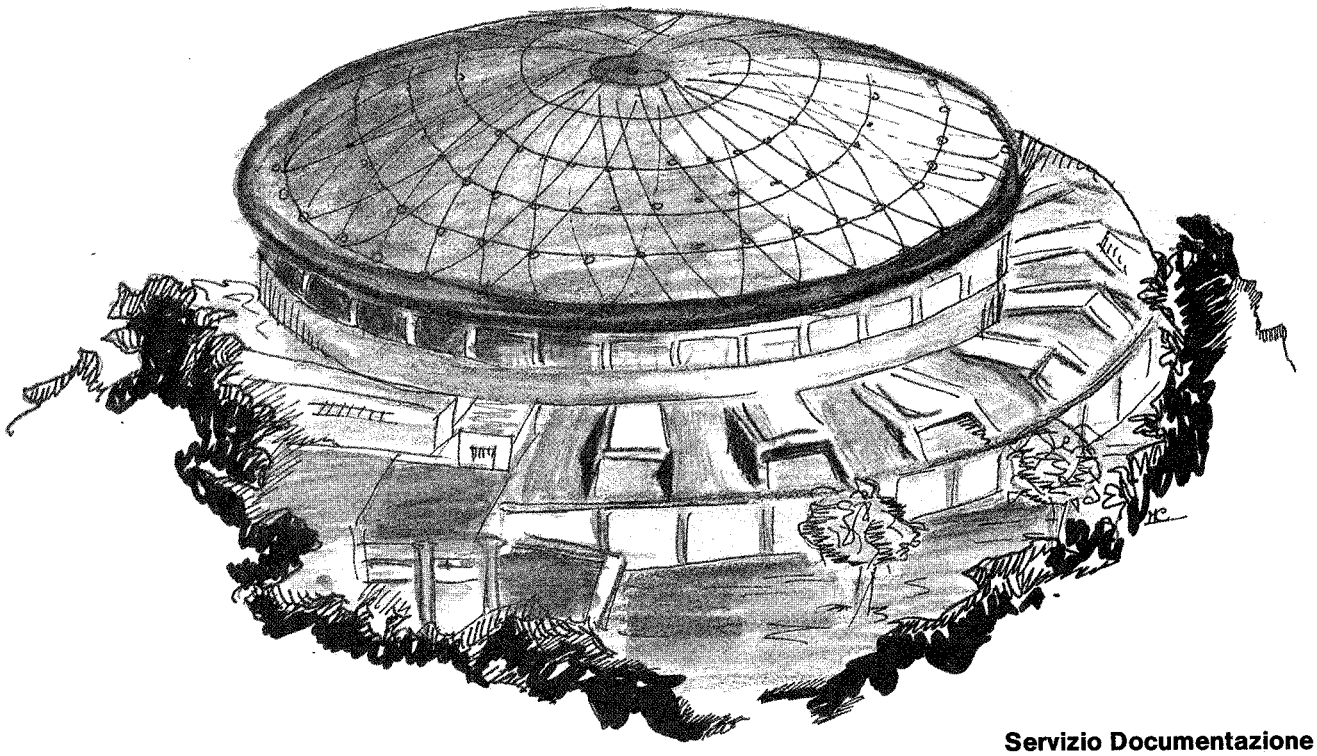

Servizio Documentazione
dei Laboratori Nazionali di Frascati
P.O. Box, 13 - 00044 Frascati (Italy)

INFN - Laboratori Nazionali di Frascati
Servizio Documentazione

LNF-90/032(P)
3 maggio 1990

THE ARGON CLUSTER-BEAM INSTALLED IN THE ADONE STORAGE RING

M. Taiuti,[1] E. Durante,[1] M. Anghinolfi,[1] N. Bianchi,[2] P. Corvisiero,[1] E. De Sanctis,[2] G. Gervino,[4] C. Guaraldo,[2] P. Levi Sandri,[2] V. Lucherini,[2] L. Mattera,[1] V. Muccifora,[2] E. Polli,[2] A.R.Reolon,[1] G. Ricco,[1] P. Rossi,[3] M. Sanzone,[1] G.M. Urciuoli,[3] U. Valbusa,[1] A. Zucchiatti[1]

[1] I.N.F.N, and Dipartimento di Fisica dell'Università di Genova, I-16146, Genova, Italy.
[2] I.N.F.N.-Laboratori Nazionali di Frascati, P.O.Box 13, I-00044, Frascati , Italy.
[3] I.N.F.N.-Sezione Sanità, I-00185, Roma, Italy.
[4] Dipartimento di Fisica dell'Università di Torino, I-10100, Torino, Italy.

The Argon cluster-beam, with maximum thickness $1.5 \cdot 10^{14}$ atoms/cm^2, installed at Frascati on the ADONE storage ring, is described. The cluster-beam works at room temperature and is used as a radiator to produce an intense tagged photon beam with energy up to 1.2 GeV. The Argon beam properties were measured using electrons stored in ADONE: the results are in good agreement with the expected values. The apparatus can produce cluster-beams of higher thickness and work with different gases. It is suitable for internal target experiments with the 1.5 GeV stored electrons.

1. - INTRODUCTION

The viability of cluster-jets as internal targets in accelerator rings has been demonstrated in a series of experiments conducted at Novosibirsk (VEP[1]), Saclay (Saturne[2]), CERN (ISR,[3] SPS[4]), Fermilab[5] and Brookhaven (AGS[5]). Other targets are beeing built at Julic (COSY[6]), CERN (LEAR[7]), and Uppsala (CELSIUS[8]) or proposed for installation in existing storage rings (PEGASYS[9] at PEP) or in new rings under construction (Novosibirsk,[10] Bates,[11] and NIKHEF[12]). These targets match very well the ring constraints of very good residual vacuum in the interaction region with the need for a reasonable high luminosity, and permit performing experiments under conditions of low background and with minimal demand for beam from primary accelerator.

In this paper we report on the Argon cluster-beam used at Frascati as internal radiator in the ADONE 1.5 GeV electron storage ring to produce an intense tagged photon beam from the bremsstrahlung of circulating electrons. The photon beam intensity is about $6 \cdot 10^7$ photons/s in the whole tagging range [$(0.4\text{-}0.8) \cdot E_0$, E_0 being the machine energy], and its energy ranges between 200 and 1200 MeV.[13]

After a brief description of the empirical scaling law used to deduce the Argon jet features from those of existing hydrogen jets (Section 2), we give a detailed description of the Argon target constructed (Section 3), and we present measured characteristics and compare them with those of hydrogen jets in the light of the scaling law (Section 4).

2. - CLUSTER-BEAM CHARACTERISTICS

A cluster-beam is produced by letting a gas, at high pressure in a vessel, expand into an evacuated chamber, through a supersonic nozzle. In this process the gas undergoes an adiabatic expansion which is described by the following equations:[14]

$$T = \Lambda^{-1}\, T_0 \qquad [^\circ K]\,, \tag{1}$$

$$p = \Lambda^{-\gamma/(\gamma-1)}\, p_0 \qquad [\text{bar}]\,, \tag{2}$$

$$v = \Lambda^{-1/2}\, M\, a_0 \qquad [\text{cm/s}]\,, \tag{3}$$

$$n = \Lambda^{-1/(\gamma-1)}\, n_0 \qquad [\text{atoms/cm}^3]\,, \tag{4}$$

$$S = \left(\frac{2\Lambda}{\gamma+1}\right)^{(\gamma+1)/2(\gamma-1)} M^{-1}\, S_0 \qquad [\mu\text{m}^2]\,, \tag{5}$$

where we have defined:

$$\Lambda = \left(1 + M^2\, \frac{\gamma-1}{2}\right), \tag{6}$$

and used the following notations: p_0, and T_0 (p, T) are the inlet (upstream) pressure, and temperature of the gas; v is the jet velocity, and

$$a_0 = \left(\frac{\gamma k T_0}{m}\right)^{1/2} = 9.12\ 10^3 \left(\frac{\gamma T_0}{A}\right)^{1/2} \qquad \text{[cm/s]} \qquad (7)$$

is the sound speed; n is the jet density, and

$$n_0 = 7.22\ 10^{21} \left(\frac{p_0}{T_0}\right) \qquad \text{[atoms/cm}^3\text{]}\ , \qquad (8)$$

is the static density; S_0 and S are the jet cross-sectional area at the nozzle throat and upstream; M is the Mach number, which is the ratio between the gas and the sound velocities; $\gamma = c_p/c_v$ is the ratio between the specific heats at constant pressure and constant volume; k the Boltzmann constant; m the gas mass; and A the atomic number.

In studies on the profile of supersonic nozzles with the same orifice diameters, Obert[15] has shown that the trumpet-shaped nozzle provides the narrowest density distribution. This nozzle consists of a converging and a diverging part, and is usually described by the throat diameter, d_1, and the cone half-angle, ϑ, of the diverging part.

During the expansion, in the converging part of such a nozzle the gas flow velocity is enhanced, while pressure and density are dropping continuosly. When, as in our case, the gas pressure at the exit of the nozzle is larger than the pressure in the expansion chamber, the subsequent development of the gas flow in the divergent part of the nozzle leads to a supersonic expansion and to a further decrease in pressure, density and temperature. In the process the Mach-number, initially equal to 0 in the stagnation volume, reaches the value of 1 near the nozzle throat and rapidily increases in the following divergent part. For suitable p_0 and T_0 values, the gas becomes supersaturated and a core forms consisting of large aggregates of molecules which move with high directionality at supersonic speed.[15] This core, selected by means of a set of collimators and a differential pumping device, travels far from the nozzle, through the residual vacuum, without absorption or diffusion by the residual gas.

The core features were studied by Hagena and Obert[17] as a function of the initial parameters (T_0, p_0), and the nozzle geometry (d_1 and ϑ) and for different gases. Cluster sizes up to 10^5 molecules/cluster were measured: the core density increases both by increasing clustering efficiency and by lowering speed. The cluster size N_{CS} can be further increased [15] by changing p_0, T_0 and d_{eq} (being $d_{eq} = C(\gamma) \cdot d_1 \cdot \cot g(\vartheta)$, where $C(\gamma)$ is a parameter which depends only on γ[17]) according to the expression:

$$N_{CS} \propto p_0\ d_{eq}^{1.5}\ T_0^{-2.4}\ , \qquad (9)$$

deduced empirically and mainly for an hydrogen beam. Moreover, Hagena and Obert[17] found that working with different gases the clusters keep the same size, no matter of the gas used, when the scaled parameters $\bar{p}_0$, $\bar{T}_0$ and $\bar{d}_{eq}$ are kept constant. That is:

$$\bar{p}_0 = \frac{p_0 \sigma^3}{\varepsilon} = \text{constant}, \tag{10}$$

$$\bar{T}_0 = \frac{T_0 k}{\varepsilon} = \text{constant}, \tag{11}$$

$$\gamma = \text{constant}, \tag{12}$$

$$\bar{d}_{eq} = \frac{d_{eq}}{\sigma} = \text{constant}, \tag{13}$$

where ε and σ are the scaling parameters for energy and length of the inter-atomic potential, and Eqs. (10)-(12) are the ground set for the "corresponding jets principle"[18], while Eq. (13) relates the beam properties to the nozzle shape.

We used Eq. (9) together with the corresponding jets principle to estimate the properties of molecular beams different from hydrogen and we developed the computer code CLUSJET[19] to optimize the shape of the nozzle as a function of the beam properties (gas, beam density, total flux, inlet pressure p_0 and temperature T_0).

3. - DESCRIPTION OF THE APPARATUS

3.1 - The cluster-jet target

In Fig. 1 is shown a picture of the Argon-target installed in the straight section n° 5 of the ADONE storage ring. The target is a vertical construction with the cluster-beam source at the top (upper cone), the interaction chamber, where the circulating electrons interact with the Argon clusters, at the center, and the jet-dump at the bottom (lower cone). Clearly visible are the turbomolecular pumps acting on the two cones and on the ADONE straight section, and the quadrupole magnets of the ring.

In Fig. 2 is reported a schematic three-dimensional internal view of the apparatus: the upper cone,V_a, contains the nozzle with its frame and the collimation system, and, the lower cone,V_b, the sinking system. Both chambers have three pumping stages, and are separated by two gating valves from the ADONE vacuum pipe V_c . The gas, that flows through the nozzle and does not cluster, is pumped off by high pumping speed devices, while the cluster core is selected using a set of four skimmers. Then the cluster-beam is collected into the sinking volume and backstreaming is reduced using a second set of four collimators.

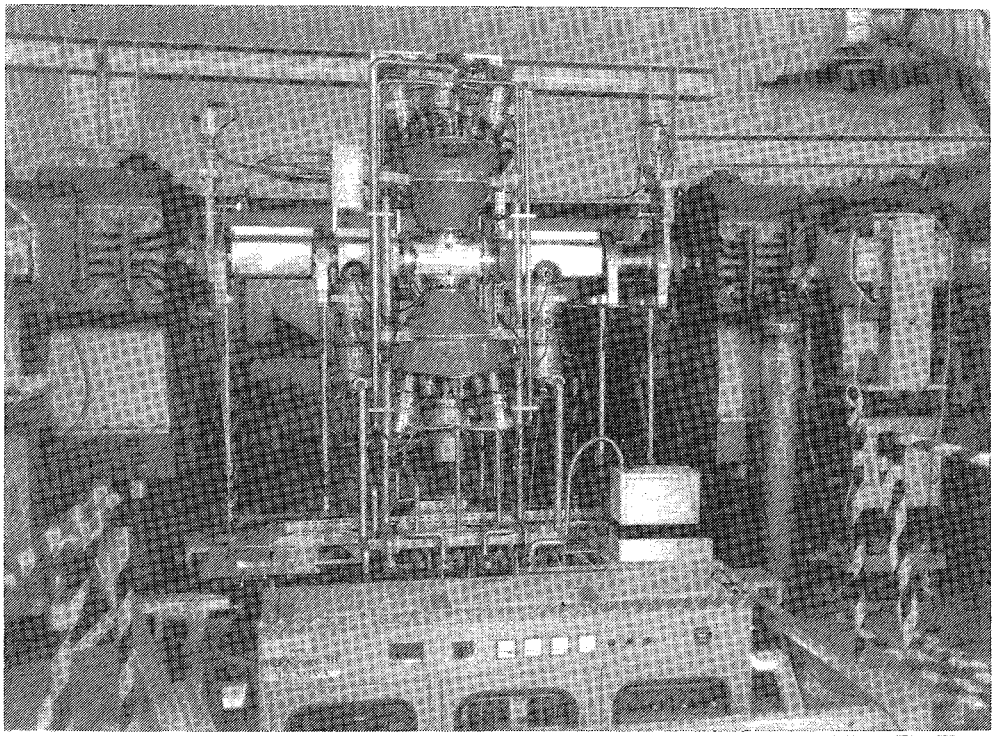

FIG. 1 - The cluster-beam target installed in ADONE. The apparatus consists of three parts: the jet injection system (the cone installed above the ring) where the jet is produced, the interaction chamber, where the molecular jet crosses the electron beam, and the jet dump (the cone installed below the ring). Also shown are the turbomolecular pumps acting on the ADONE straight section and the machine quadrupole doublets.

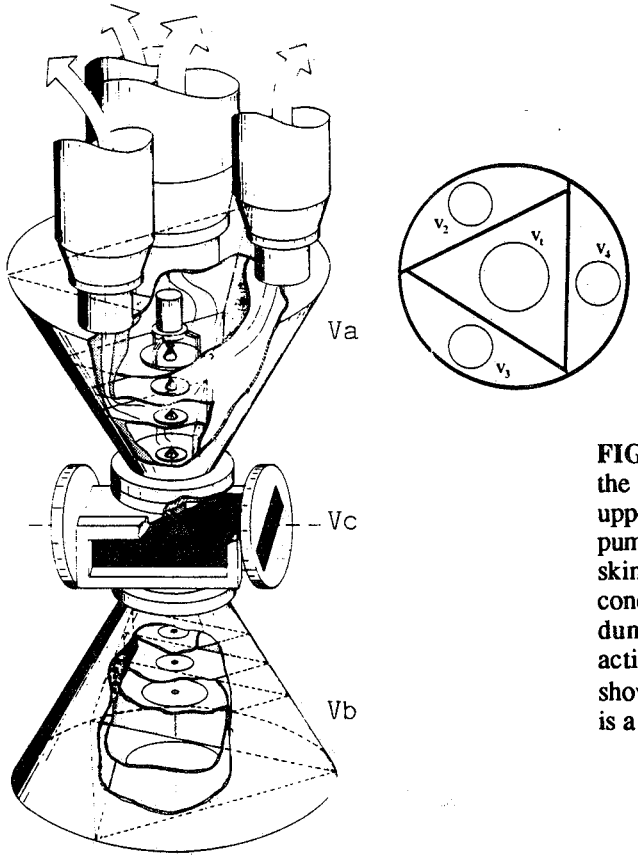

FIG. 2 - Three-dimensional view of the ultra high vacuum chamber: the upper cone contains the differentially pumped beam source, with the nozzle, skimmers and collimators; the lower cone, the differentially pumped beam dump.The turbomolecular pumps acting on the upper cone V_a are shown. The draw on the top-right side is a section of the cone base.

The target design and the molecular beam parameters were determined according to the following constraints: *i)* need to limit the pressure increase in the ADONE vacuum pipe below $5 \cdot 10^{-7}$ mbar; *ii)* need to produce negligible effects on the circulating beam quality, *iii)* need to provide for a total bremsstrahlung photons yield lower than 10^8 photons/s, in order to keep at an acceptable low level the ratio of the random to real coincidences in the tagging counters[13], and *iv)* need to keep the space around the scattering chamber as free from equipment as possible, to allow for external detectors of the reaction products.

Constraint *i)* required the separation of both the expansion and sink chambers from ADONE vacuum pipe by three stages of differential pumping, realized with turbomolecular pumps, and by using suitable skimmers.

Constraints *ii)* and *iii)* limited the jet thickness below 10 ng/cm^2 which, as shown in Ref. 20, do not affect the beam quality and provide the maximum tollerated photon intensity for an average stored current of 60 mA.

Constraint *iv)* suggested the double conical shape shown in Fig. 1: nearly the whole horizontal plane and a vertical angle of $\pm$ 66° is left free for detectors and other experimental equipments. To maintain good conductances inside the vacuum chambers, the cone bases were minimized, and the turbomolecular pumps were mounted at 9° 45' from vertical.

3.2 - The vacuum system

The Ultra High Vacuum (UHV) chambers were realized in AISI 316L steel by Costruzioni Saldate Collaudate (CSC) -Schio. The upper and lower chambers V_a and V_b were built out of the same drawing: the outer lateral surface is a 3 mm steel foil soldered on a 10 mm steel base of 640 mm diameter. A tetrahedron 5 mm thick and with equilateral base was placed inside the cone in such a way that the three edges were soldered on the inner conical surface and the base edges on the cone base. Thus the cone volume is divided into four parts: one inside the tetrahedron (V_t) and three obtained from the residual volume (V_2, V_3, V_4) [The section of the cone's bases is schematically drawn in Fig. 2]. The tetrahedron was then cut from the top by three horizontal planes 10 mm thick, 35 mm far from each other to select four volumes. The main one (V_1), being the lower part of the tetrahedron, is connected with open air through the cone base, while the others are connected with V_2, V_3 and V_4, respectively, through rectangular holes in the tetrahedron lateral surfaces. V_1 is connected with open air through several conflact flanges (CF): specifically one CF200, one CF63 and eight CF35 , while V_2, V_3, V_4 are connected through one CF150 and two CF35 each.

We used turbomolecular pumps directly flanged to the relevant vacuum vessels in order to make easy repair and service and to reduce the loss of pumping speed due to the limited conductance of the vacuum pipe. The connections are the following: on the CF200 a turbomolecular pump model LH TURBOVAC 1000, on each CF150 a turbomolecular pump model LH TURBOVAC 360, on the CF63 a cold head LH RG20. Each volume has one LH IE 220 ionization gauge for measurements in the range (10^{-10} - 10^{-2}) mbar and one Infrared lamp

Luminy Instruments LE14.1 with 1.4 KW maximum power to provide a constant heating of the inner surfaces. In the upper cone V_a, the volumeV_1 was further connected to one LH TR 205 Pirani gauge tubes for residual pressure measurements in the range 10^{-3} mbar - 10^{+3} mbar, one UHV tubular feedthrough for the gas inlet, one UHV current leadthrough with five steel conductors and five constantan conductors for the temperature gauge signals, and one UHV rotary leadthrough for the jet pulsing system.

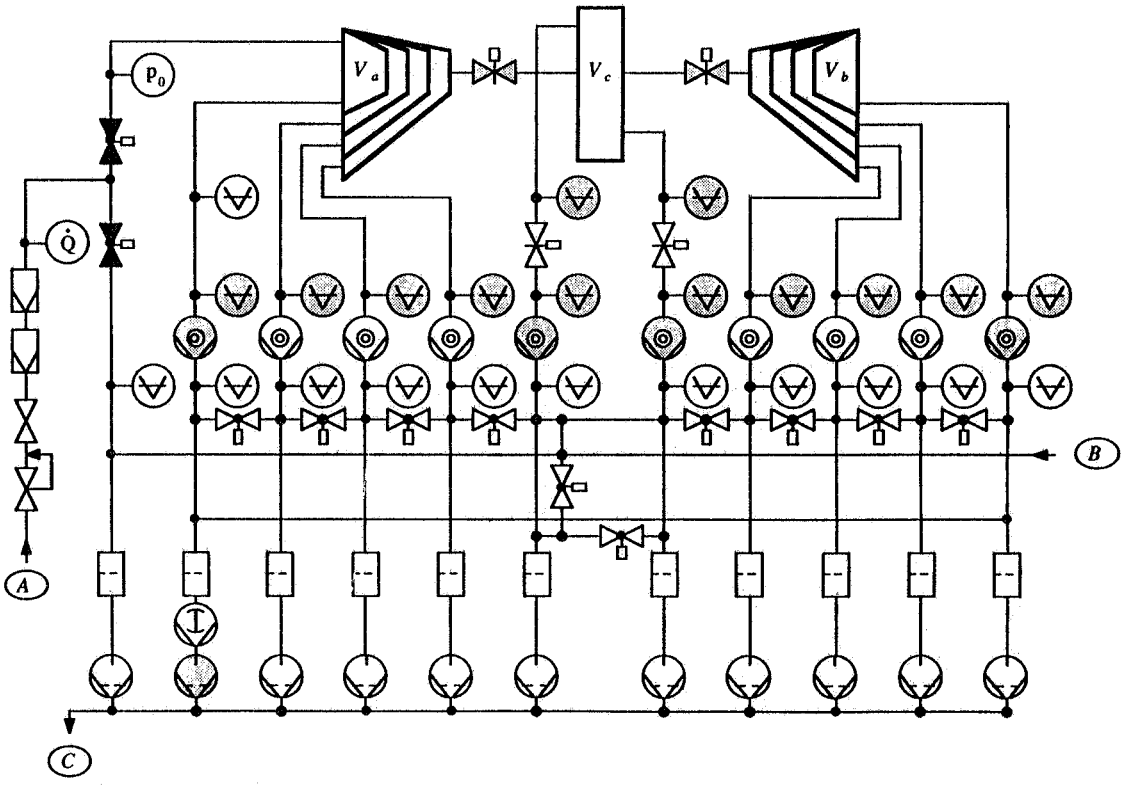

FIG. 3 - Pumping system, gas flow and venting set-up. The gas flows from *A* through the upper cone V_a, the ADONE vacuum pipe V_C and the lower cone V_b. The residual gas is pumped off toward *C*. In the venting operation N_2 flows from *B* inside the vacuum chamber.

In Fig. 3 the whole pumping system scheme is reported: each turbomolecular pump is connected to a LH TRIVAC-B D25B rotary pump with 25.7 m^3/h pumping speed and 10^{-4} mbar ultimate pressure. The first stage of the differential pumping system is connected to a LH RUVAC WSU500 coupled to a LH TRIVAC-B D40B rotary pump with 40 m^3/h pumping speed and 10^{-4} mbar ultimate pressure. A supplementary LH TRIVAC-B D25B rotary pump is connected to the gas line to provide for a fast evacuation when the used gas is changed. The forevacuum is measured by LH TR201 Pirani gauge tubes. All the forevacuum lines are connected in cascade by LH straight-through electropneumatic valves DN25KF used in the venting procedure and to connect more turbomolecular pumps when the corresponding rotary pump breaks down.

As said above, two fast acting UHV all metal valves (VAT ∅ = 25 mm) separate the production and sink chambers from the ADONE vacuum pipe to easy the jet on/off operations and to prevent the possible contamination of the ring in case of a large pressure bump due to breakdown of the target system. These two valves were soldered on the ADONE vacuum pipe V_c

in order to reduce the distance between the nozzle and the interaction point. The upper and lower cones are connected to the volume V_c with two CF200 flanges.

The target vacuum system is able to locally confine the gas to a high degree and recover the ring base pressure in a short distance both upstream and downstream from the target. Such increases in the base pressure would add to the effective target thickness and decrease the lifetime of the recirculating beam. In order to contain the pressure rise each time the jet is fired, and to return quickly to normal vacuum levels when the jet is switched off, two LH TURBOVAC 1000 turbomolecular pumps were located on the straight section immediately before and after the interaction chamber. These pumps are connected through a VAT 10 CF200 electropneumatic gate valve whose movement is controlled by a couple of LH IE220 vacuum gauges. The pumping in the rest of the ring is performed by the existing turbo pumps.

3.3 - The nozzle

The trumpet-shaped nozzle for the Argon jet (Fig. 4) was designed using the results of the CLUSJET code with the following requests: *i)* nozzle diameter $\bar{d}_{eq}$ equal to those in Refs. [3] and [15] and length corresponding to M = 26 at the nozzle end, *ii)* a total throughput upper limit equal to 8 mbar·l/s, since the adopted differential pumping system cannot work properly at higher intensities, and *iii)* capability of producing a high density molecular beam at room temperature.

Three copper nozzles with 50 μm, 70 μm and 80 μm nominal diameter and $\theta = 3.5°$ semiaperture were manufactured at CERN; the first two skimmers were produced by Beam Dynamics Inc. while the others by CSC. The nozzle and the four skimmers were mounted on the same frame, within a 10 μm tolerance. The frame can be easily removed from the volume V_a through the CF200 flange where the 1000 l/s turbomolecular pump is placed.

The beam diameter, at the interaction point, located 25 cm far from the nozzle, is mechanically fixed by the skimmer's geometry, because, as shown in Refs. [15] and [21], molecular beams without collimation have constant density within a cone of $\theta \leq 2.5°$ semiaperture.

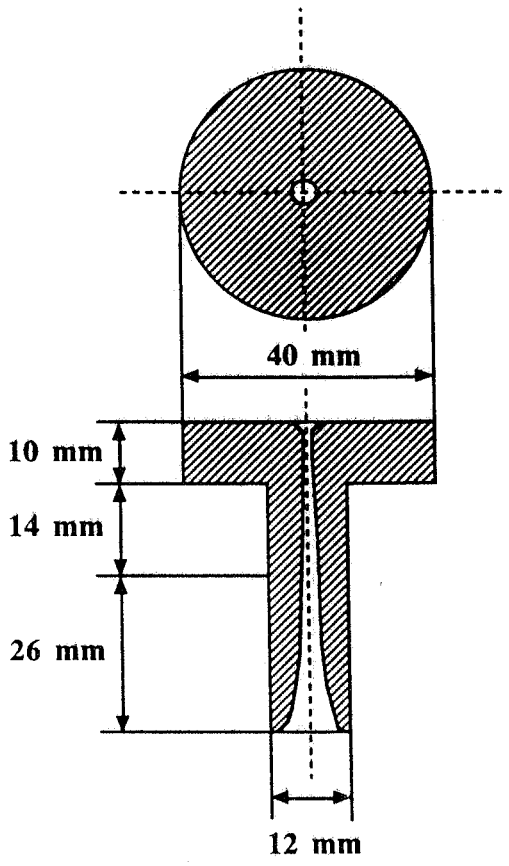

FIG. 4 - The trumpet-shaped nozzle.

3.4 - Control system

The control of the beam parameters relied on the measurement of the gas inlet temperature, T_0, and pressure, p_0, the residual vacuum p_r in the sinking volume, and the total throughput $\dot{Q}$. This latter, from Eqs. (3)-(5), is related to the inlet parameters by the relation:

$$\dot{Q} = n(M)\, v(M)\, S(M) = 5.19\, 10^{17}\, \gamma^{1/2} \left(\frac{2}{\gamma+1}\right)^{(\gamma+1)/2(\gamma-1)} \frac{p_0\, {d_1}^2}{(T_0\, A)^{1/2}} \quad [\text{atoms/s}]\,, \qquad (14)$$

that, for a given temperature, shows a linear dependence from p_0 with a slope proportional to the square of the nozzle throat diameter, ${d_1}^2$.

The temperature T_0 was measured by a 4-wires platinum resistance, the pressure p_0 by a MKS manometer with 1.5 % uncertainty, and the total throughput $\dot{Q}$ by a TELEDYNE-HASTINGS flowmeter with 0.1 % resolution. No regulation was available for the temperature T_0, while the pressure p_0 was regulated by a TESCOM motor actuated pressure reducing regulator with 5 p.s.i. resolution.

The apparatus can produce, with minor changements, Argon cluster-beams with higher thickness or cluster-beams of lighter mass number gases. In fact, from Eqs. (9) and (14), it is clear that at $\dot{Q}$ constant, the cluster size is mainly a function of $T_0^{-1.9}$. Therefore, it is possible to increase the jet density by simply lowering the inlet temperature without any modifications in the pumping system. The T_0 lower limit can be obtained imposing that the gas clusters at M>1, that is after the nozzle throat, to avoid occlusions of the throat itself. In these conditions the Argon cluster-beam could work at T_0 down to 110 °K with a gain of 10 in density.

The apparatus was automatically controlled by a dedicated computer (Programmable Multifunction Controller by ORSI Automazione) which performed all the standard and emergency switch on-switch off procedures, the cluster-beam density regulation, and the recording of the measurements.

4. - RESULTS

Here, we report on the results of measurements of the Argon cluster-jet characteristics performed in the following operating conditions: inlet pressure and temperature 1÷20 bar and about 300 °K, respectively; nozzle throat diameter 70 μm and semiaperture 3.5°. In Table I are reported the diameters and conductances of the used skimmers, together with the measured residual vacuum values of each stage of the differential pumping device for a cluster-beam density equal to 10 ng/cm^2. From a total flux of $\approx 10^{20}$ Ar-atoms/s expanding from the nozzle, the collimator system selected about 10^{17}-10^{18} atoms/s, which corresponds to a target thickness of 1÷10 ng/cm^2 (∅=6 mm) on the path of the electron beam (that is at a distance of ≈25 cm from the nozzle).

TABLE I - Diameters of the adopted skimmers, estimated conductances, pumping speeds, and measured residual pressures corresponding to a 10 ng/cm^2 Argon cluster-beam.

	Upper cone (V_a)				Interaction chamber (V_c)	Lower cone (V_b)			
Stage	V_1	V_2	V_3	V_4		V_4	V_3	V_2	V_1
Skimmer diameter (mm)	1.1	2.2	3.9	5.5		15	16	18	19
Conductance [l/s]	0.1	0.4	1.2	2.5		21	26	30	36
Pumping speed [l/s]	700	250	250	200	2000	200	250	250	1400
Measured pressure (mbar)	$6.5\cdot10^{-2}$	$1.3\cdot10^{-2}$	$2\cdot10^{-5}$	$3.5\cdot10^{-6}$	$4\cdot10^{-7}$	$2\cdot10^{-6}$	$5\cdot10^{-6}$	$4.8\cdot10^{-2}$	10^{-4}

4.1 - Nozzle diameter and skimmer's geometry

The effective nozzle throat diameter was derived from measurements of the temperature T_0, pressure p_0 and total throughput Q_0. During the preliminary tests, the nozzle throat was occluded by impurities and had to be cleaned several times. Every time the effective diameter, as determined from Eq. (14), resulted slightly different with measured values ranging between 55 μm and 68 μm. This problems was eliminated placing a Nupro 0.5 μm sintered filter just before the nozzle.

The throughput of the target system was mainly defined by the pumping in the first stage, which, referring to Table.I, takes the highest gas load. For a fixed cluster fraction and geometry, the amount of pumping on this stage defined the maximum throughput of the system and thus the ultimate density of the jet. From Table I, it results also that the geometry of skimmers is such that all the gas flowing through the interaction chamber, V_c, reached the volume V_1 in the sinking cone.

4.2 - Vacuum levels

Fig. 5 shows the vacuum levels measured, in different runs and for various Argon jet thicknesses, in the straight section where the jet-target is installed. The pressure rise up to about $5\cdot10^{-7}$ mbar in the vacuum pipe around the target region was mainly due to the clusters which did not reach the sink system. The vacuum in the rest of the ring resulted unaffected. The recovery time to the normal vacuum level $6\cdot10^{-10}$ mbar, after the jet was switched off, was about one minute. Furthermore, by comparing the mass spectra from the ADONE residual gas in normal condition and after switching the jet off, we found no changement in the composition of the residual gas.

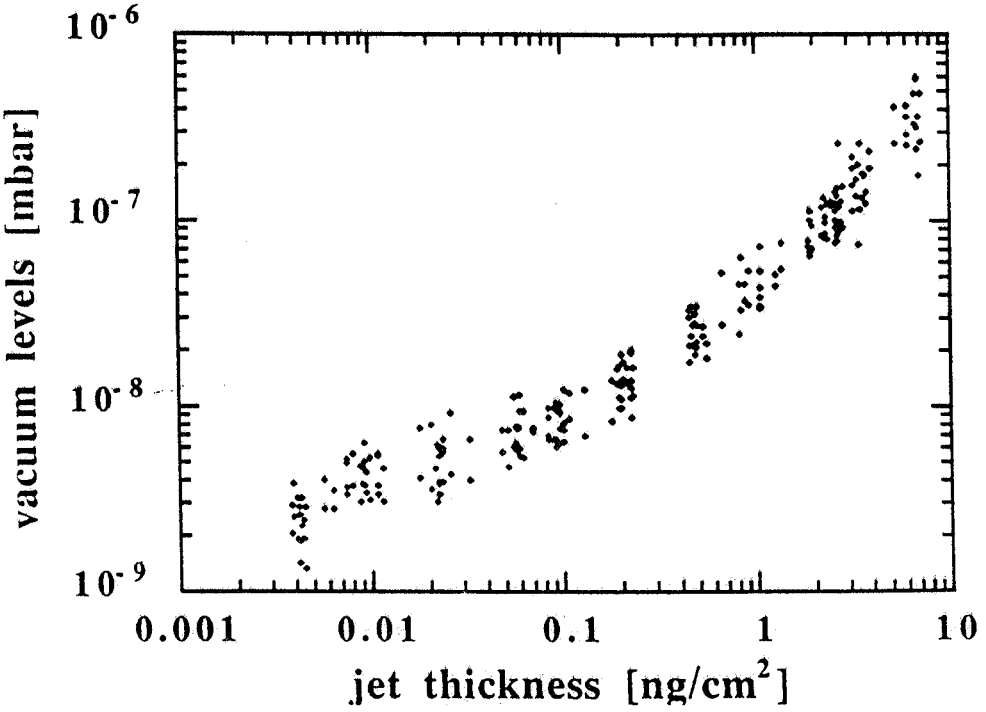

FIG. 5 - Vacuum levels in the straight section where the jet target is installed versus the jet thickness.

4.3 - Jet diameter

The jet diameter d_{ip} at the interaction point was measured by moving the electron beam radially, while keeping its trajectory parallel to the straight section axis within 0.1 mm uncertainty, and recording the rate of the tagging counters. We performed several measurements at different electron energies and jet densities, and over the range -12 mm $\leq x_d \leq$ 10 mm (x_d being the radial displacement of the electron orbit from the central one) for which the efficiency loss of the tagging detector is negligible.[22] The electron beam intensity distribution is a gaussian centered at x_d with an intrinsic radial standard deviation σ whose values are 0.6 mm and 1.8 mm, respectively at 500 and 1500 MeV. In the hypothesis of uniform density and cylindrical shape, the jet diameter d_{ip} is related to the tagger counting rate $c(x_d)$ by the convolution:

$$c(x_d) \propto \int_{\frac{-d_{ip}}{2}}^{\frac{d_{ip}}{2}} e^{-(x-x_d)^2/2\sigma^2} \left(\left(\frac{d_{ip}}{2}\right)^2 - x^2\right)^{1/2} dx \ . \qquad (15)$$

In Fig. 6 are shown the beam profile of the Argon cluster-beam, measured at the given electron energies and jet densities. The obtained diameter values agree very well among each other: their average value is $d_{ip} = (5.4 \pm 0.1)$ mm.

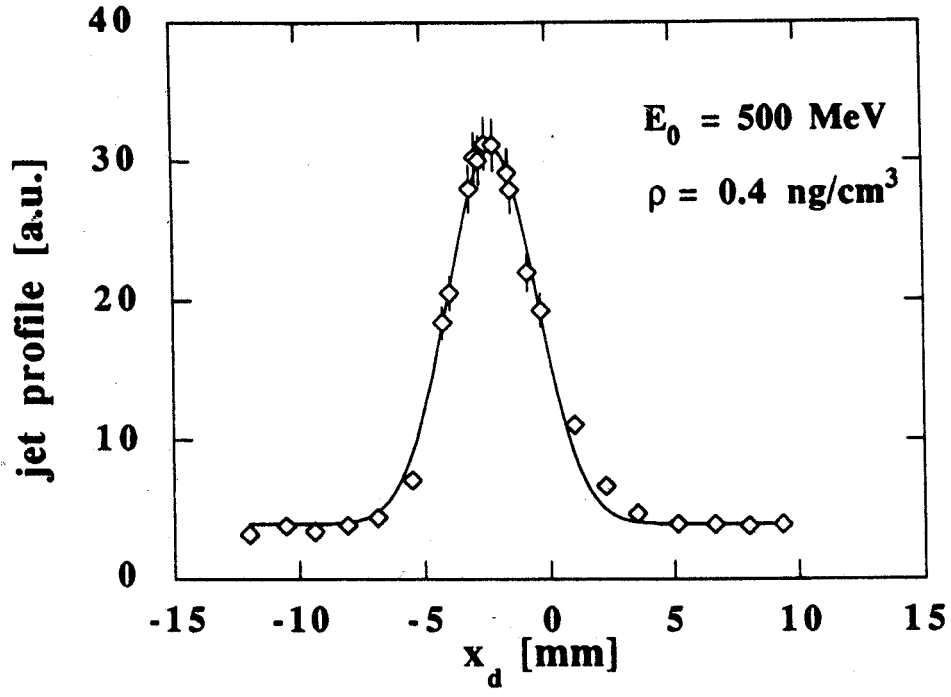

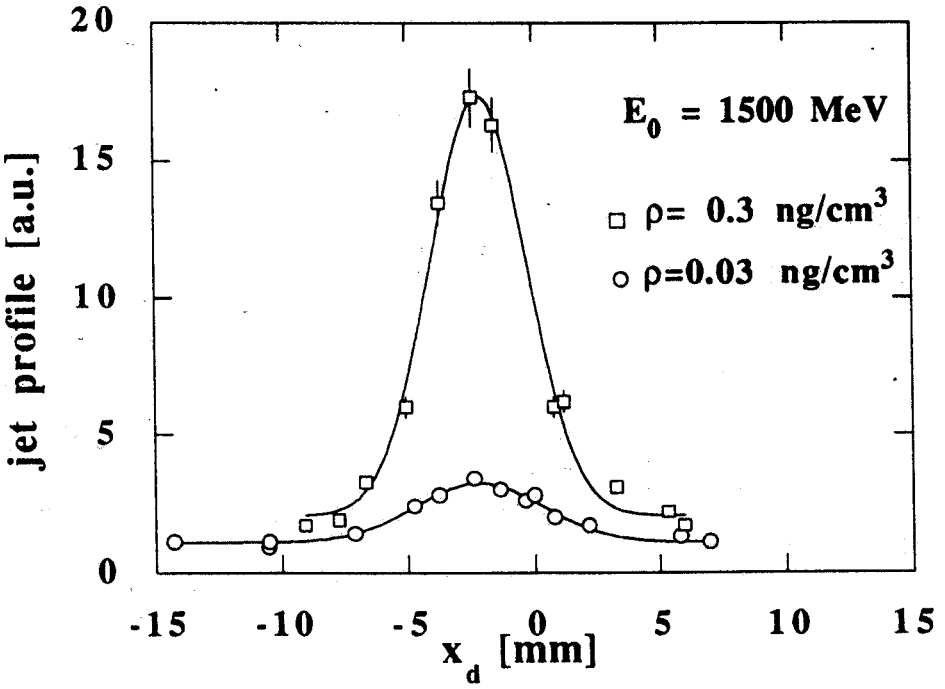

FIG. 6 - Jet profiles measured at the given electron energies and jet thicknesses. The solid line curve are the best fit ($\chi^2 = 2.24$) obtained from Eq. 15 with $d_{ip} = 5.4$ mm.

4.4 - Jet density

The jet density at the interaction point was monitored on line using the expression:

$$\rho = \frac{m\dot{q}}{S_{ip} v_\infty} \qquad [g/cm^3] , \qquad (16)$$

where S_{ip} ($=\frac{\pi}{4} d_{ip}^2$) is the molecular beam section at the interaction point, v_∞ is the beam velocity, which in the hypothesis of supersonic expansion (M » 1) is given by:

$$v_\infty = \left(\frac{2\gamma}{\gamma-1} \right)^{1/2} \left(\frac{kT_0}{m} \right)^{1/2} \qquad [cm/s] , \qquad (17)$$

and $\dot{q}$ is the cluster-beam intensity. This is equal to the throughput of the sinking volume which is given by:

$$\dot{q} = 2.4 \cdot 10^{19} \, v_t \cdot p_r \qquad [atoms/s]. \qquad (18)$$

where v_t [l/s] is the evacuating pumping speed in the sinking chamber.

In Fig. 7 the target thickness, deduced from the measured residual vacuum p_r by using Eqs. (16) and (18), is plotted as a function of the inlet pressure p_0. As it is shown, the transition from gas- to cluster-jet occurs for an inlet pressure of about p_{cb}=5.5 bar, and produces a sudden increase on the jet density. The beam density, for pressure values above p_{cb} corresponding to the cluster-beam regime, grows linearly as p_0 increases. The dashed curve is the CLUSJET result: it has the same behaviour than experimental points, but is systematically higher. Moreover, from the analysis of the measured p_{cb} value performed with the code CLUSJET, it resulted that the transition occurs at a Mach number value M≈3.

The jet thickness values deduced from Eq. (16) were verified measuring the mean lifetime τ of the electron stored in ADONE, which is related to ρ by:[20]

$$\tau = \frac{t_0}{\sigma_\varepsilon \rho \, d_{ip}} , \qquad (19)$$

where t_0 is the revolution time of the circulating electrons, and σ_ε the removal cross section. In our case, as shown in Ref. 20, σ_ε involves only those processes of bremsstrahlung in which electrons lose sufficient energy to place them outside the acceptance band-width ε of the ring (ε=0.01·E_0). The jet thickness values deduced from such measurements are also shown in Fig. 7 as open circles: they are in good agreement with those derived from the residual vacuum in the sinking volume.

Because the removal cross section involves only the bremsstrahlung processes, the electron beam lifetime for a jet-target of atomic number Z would be proportional to $\rho \cdot Z^{-2}$. This is shown in Fig. 8 where are plotted the limiting density and luminosity available at ADONE with different

gases (A is the gas atomic number) for 20 minutes beam lifetime, and for 100 mA stored electrons. As it is seen, the maximum luminosity per nucleus is about 10^{33} Z^{-2} $cm^{-2}s^{-1}$ which is more than sufficient to carry out electron scattering experiments, particularly when using large solid angle detectors.[13]

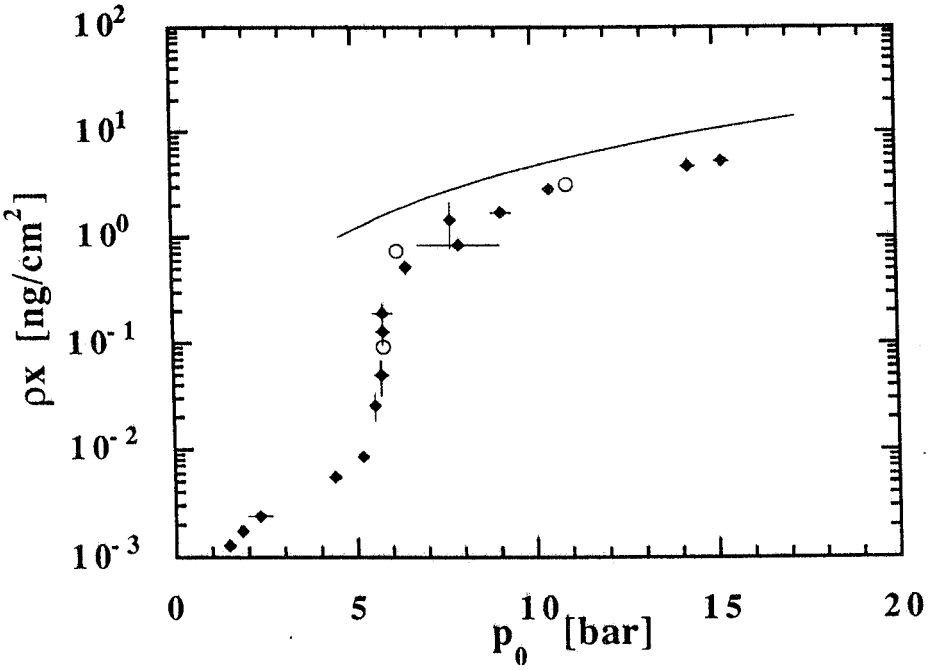

FIG. 7 - Target thickness ρx vs. inlet pressure p_0 measured with the d_1 = 70 μm diameter nozzle, a 0,5 μm sintered filter, and the Ø=1.1 mm first skimmer. Solid circles: thicknesses deduced from measurements of the residual vacuum in the sinking volume; open circles: values derived from beam lifetime measurements. The dashed line curve is the result of the CLUSJET code.

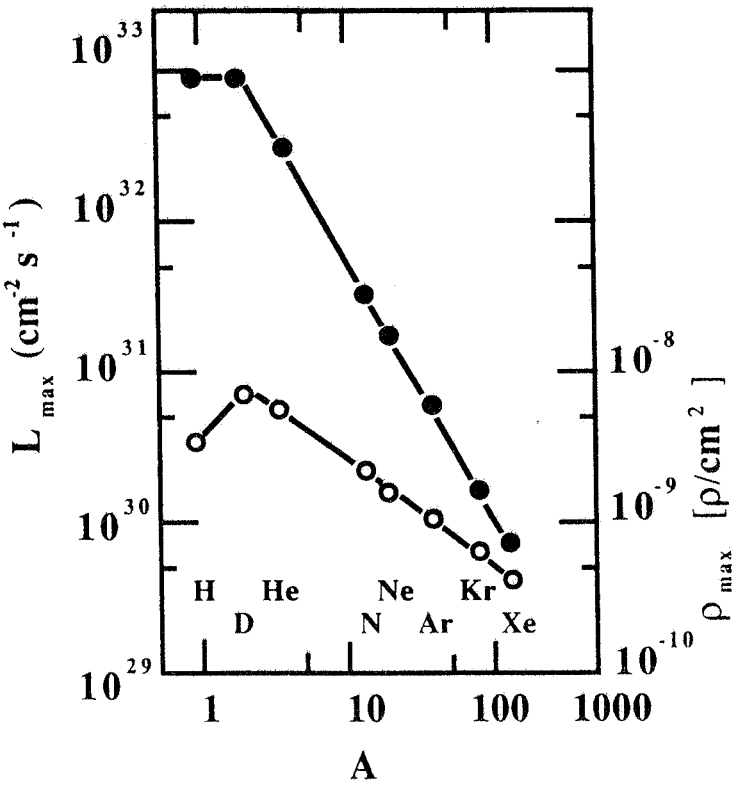

FIG. 8 - Calculated maximum luminosity for a 20 minutes beam lifetime (upper curve and left ordinate scale) and the target density (lower curve and right ordinate scale) as a function of the atomic weight A.

5. - CONCLUSIONS

We have described the Argon jet installed in the ADONE storage ring. The cluster-beam features were derived from the already working hydrogen condensed beams by means of the CLUSJET code, and are well described by the corresponding jets principle and the scaling law.

The cluster-jet, after its installation in the ADONE storage ring, was used for a total period of a month over a year and during this period its properties were well reproduced within a few percent fluctuations. A presure rise up to about $5 \cdot 10^{-7}$ mbar in the vacuum pipe around the target region was measured. The vacuum in the rest of the ring resulted unaffected. The recovery time to the normal vacuum level, after the jet was switched off, was about one minute. No changement in the mass spectrum of the residual gas was observed.

The operating conditions were: inlet pressure and temperature (1÷20) bar and about 300 °K, respectively; nozzle throat diameter 70 μm and semiaperture 3.5°. From a total flux of $\approx 10^{20}$ Ar-atoms/s expanding from the nozzle, the collimator system selected about ($10^{17} \div 10^{18}$) atoms/s, which corresponds to a target thickness of (1÷10) ng/cm^2 (∅=6 mm) on the path of the electron beam.

The apparatus can work at lower temperatures and with different gases. Luminosities per nucleus of about $10^{33} \cdot Z^{-2}$ cm^{-2}s^{-1} are achievable with 20 minutes lifetime and good emittance for 100 mA circulating electrons of energy up to 1.5 GeV.

We gratefully acknowledge the members of the Jet Target groups at Frascati and Genova (M. Albicocco, E. Cavanna, L. Falco, U. Lantero, A. Macioce, A. Manco, A. Orlandi, W. Pesci, A. Rottura, and A. Viticchié) for the continue assistance in all stages of construction, installation, and testing of the Argon-jet apparatus. Moreover, we express our gratitude to Dr. V. Chimenti for valuable advice and assistance for vacuum problems.

REFERENCES

[1] S.G.Popov, in Proc. of the Workshop on the Use of Electron Rings for Nuclear Physics Research, Lund, October 5-7 1982, Eds. J.O. Adler and B. Schrøeder (1982), p. 150; V.F. Dmitriev et al Phys. Lett. **157 B** (1985) 143, and Nucl. Phys. **A464** (1987) 181, and M.V. Motsovoy et al. Phys. Lett. **188 B** (1987) 181.

[2] R.Burgei, M.Garçon, M.Grand, B.Gonel, R.Maillard, A.Malthiery and J.Martin Nucl. Instr. and Meth. **204** (1982) 53.

[3] M.Macrì, in Proc. of the Workshop on Physics with Low Energy Cooled Antiprotons, Plenum, New York, 1983, p.432; and C. Baglin et al., Phys. Lett. **172 B** (1986) 455, and C. Baglin et al., Nucl. Phys. **B286** (1987) 592.

[4] L.Dick and W.Kubischta, in Proc. of the School on Hadronic Physics at Intermediate Energies, Folgaria, February 17-22 1986, Eds. T.Bressani, and R.A.Ricci,.North Holland, 1986, p.209; and A. Bernasconi et al. Phys. Lett. **206 B** (1988) 163.

[5] B.C. Stringfellow, A.T.Bujak, D.D.Carmony, Y.H.Chung, J.E.Finn, L.J.Gutay, A.S. Hirsch, M.Mahi, G.L.Paderewski, N.T.Porile, T.C.Sangster, and R.P.Scharenberg, F. Turkot, Nucl. Instr. and Meth. **A 251** (1986) 242.

[6] D. Prasuhn in Proc. of the Topical Conference on Electronuclear Physics with Internal Targets, SLAC January 9-12 1989, Ed. G.Arnold, World Scientific, 1990, p.153; and F.Hinterberger, T.Mayer-Kuckuk and D.Prasuhn, Nucl. Instr. and Meth. **A 275** (1989) 239.

[7] M.Macrì, in Proc. of the CERN Accelerator School, Antiprotons for Colliding Beam Facilities, 11-21 October 1983, Eds. P. Bryant and S. Newman, CERN 84-15 (1984), p.469.

[8] C.Ekström, in Proc. of the Topical Conference on Electronuclear Physics with Internal Targets,SLAC January 9-121989, Ed. G.Arnold, World Scientific, 1990, p.171.

[9] K. Van Bibber, Nucl. Instr. and Meth. **B 40/41** (1989) 436.

[10] S.G. Popov,in Proc. of the Topical Conference on Electronuclear Physics with Internal Targets,SLAC January 9-121989, Ed. G.Arnold, World Scientific, 1990, p.37

[11] S.Kowalski, ibidem, p. 48.

[12] C.W. de Jager, ibidem, p. 55.

[13] E. DeSanctis, et al. in Proc. of Perspectives on Theoretical Nuclear Physics, Cortona 16-18 October, 1989, Eds. L. Bracci et al., p. 75; and Frascati Internal Report LNF-90/001 (P).

[14] D.Shapira, J.L.C.Ford Jr., R.Novotny, B.Shivakumar, R.L.Parks and S.T.Thornton, Nucl. Instr. and Meth. **228** (1985) 259.

[15] W. Obert - "Properties of Cluster-beams formed with Supersonic Nozzles", Proc. of the 11th Int. Symp. on Rarefied gas dynamics, Cannes (July 1978).

[16] H.W. Becker, L. Buchmann, J. Görres, K.U. Kettner, H. Kräwinkel, C. Rolfs, P. Schmalbrock, H.P. Trautvetter and A. Vlieks, Nucl. Instr. and Meth. **198** (1982) 277.

[17] O.F.Hagena and W.Obert , J. Chem. Phys. **56** (1972) 1793.

[18] J.O.Hirschfelder, C.F.Curtiss and R.B.Bird, Molecular Theory of Gases and Liquids, Wiley, New York, 1954.

[19] M.Taiuti et al., Frascati Internal Report, to be published.

[20] V.Muccifora et al., Frascati Internal Report, LNF 90/022 (P), submitted to Nucl. Instr. and Meth.; and M.Taiuti, et al, Frascati Internal Report, to be published.

[21] J.Gspann in Proc. of the Workshop on the Use of Electron Rings for Nuclear Physics Research, Lund, October 5-7, 1982, Eds.J.O. Adler and B. Schrøeder; (1982)p 85.

[22] V.Muccifora and E.DeSanctis, Frascati Internal Report LNF 86/30 (1986).